ELSEVIER

X-ray tomography of whole cells

Mark A Le Gros[1], Gerry McDermott[1] and Carolyn A Larabell[1,2]

X-ray tomography has been shown to provide insights into the internal structure of whole cells that can't be obtained by any other means. With recent advances in instrumentation and the advent of automated cryogenic sample stages, it has become possible to collect isotropic tomographic data from radiation-sensitive cells and to compute reconstructions with a high degree of fidelity to a resolution of 50 nm. The new generation of X-ray optics will extend this resolution limit to 15 nm or better. The development of X-ray tomography of whole cells generates opportunities to study cells, and cellular processes, in a completely new way.

Addresses
[1] Physical Biosciences Division, Lawrence Berkeley National Laboratory, 1 Cyclotron Road, MS 6-2100, Berkeley, CA 94720, USA
[2] Department of Anatomy, University of California San Francisco, 513 Parnassus Avenue, San Francisco, CA 94143, USA

Corresponding author: Larabell, Carolyn A (larabel@itsa.ucsf.edu)

Current Opinion in Structural Biology 2005, **15**:593–600

This review comes from a themed issue on
Biophysical methods
Edited by Wah Chiu and Keith Moffat

Available online 8th September 2005

0959-440X/$ – see front matter

DOI 10.1016/j.sbi.2005.08.008

Introduction

X-ray tomography is applicable over a wide range of size scales encountered in biology. At the larger end of the scale, tomography is well established as a tool for medical imaging. For example, CAT (computer-assisted tomography) is now a commonplace procedure. At a smaller size scale, significant success has been seen with the internal imaging of biostructures, such as bone and soft tissues [1,2]. Recently, with the publication of X-ray tomograms of whole cells showing cellular and subcellular structures at a resolution of ~40 nm, X-ray tomography advanced to the next level of scale [3••,4,5]. Recent developments in X-ray optics have demonstrated that, in the near future, resolution will be extended to a limit of better than 15 nm [6••]. The development of automated cryogenic sample stages has opened up the possibility of collecting a complete tomogram and then immediately moving another cell into the field of view, without having to change or otherwise adjust the sample holder. As the process of aligning the sample and taking a complete data set takes less than three minutes, tomographic reconstructions can be generated in statistically significant numbers — essential when correlating phenotypic or morphological changes in the cell with genetic/biochemical information or data from other types of microscopy.

The high penetrating power, coupled with a near absence of reflection at the interface of dissimilar materials, makes X-rays an ideal probe for studying the morphology and composition of labeled proteins in single cells [7,8]. Moreover, as the wavelengths are short, this can be done at relatively high resolution. The occurrence of specific elemental absorption lines also allows imaging to be performed under conditions in which organic material has ten times more contrast than water [9]. This region of the X-ray spectrum is the so-called 'water window', and lies between the absorption edges of carbon and oxygen at 284 and 534 eV, respectively. Water layers up to 10 μm thick can be penetrated, whereas organic cell structures are visualized with good contrast. Inorganic materials, especially those containing electron-dense elements, are observed with even better contrast. This opens up the possibility of their use as markers, especially when conjugated to antibodies or other macromolecule-specific tags. In such instances, the position of high-contrast labels can be determined with much better resolution than that observed for organic cell contents. This holds the promise of generating 'tomographic atlases' that chart the spatial and temporal location of individual proteins and macromolecular complexes at every stage during the cell cycle.

In addition to the above-mentioned full-field microscopy techniques, other novel X-ray imaging methods, such as coherent diffraction imaging, are currently being developed and are beginning to find application in whole-cell imaging.

In combination with existing microscopy methods, these new X-ray techniques can provide unique insights into the workings of the cell. This review discusses progress in X-ray tomographic imaging of whole cells that has occurred over the past three years.

Recent progress in instrumentation and techniques

The instruments of cellular X-ray tomography fall into two clear categories: microscopes that require optics such as zone plates and microscopes that don't require any focusing optical elements. In terms of the former, there are two main types of zone plate based microscopes: full-field transmission X-ray microscopes (TXMs) and scanning transmission X-ray microscopes (STXMs).

Microscopes that don't require focusing optics are classified as lensless projection imaging microscopes (PIMs) or diffraction imaging microscopes (DIMs). The sources of X-rays for TXM and PIM can, in principle, be laboratory sources, such as laser plasma sources or rotating anodes. However, for the best results from all of these imaging techniques, synchrotron bend magnets or insertion devices such as an undulator must be used.

Zone plate based microscopes

Of the two common configurations of zone plate based X-ray microscopes, TXM can take images much faster than

Figure 1

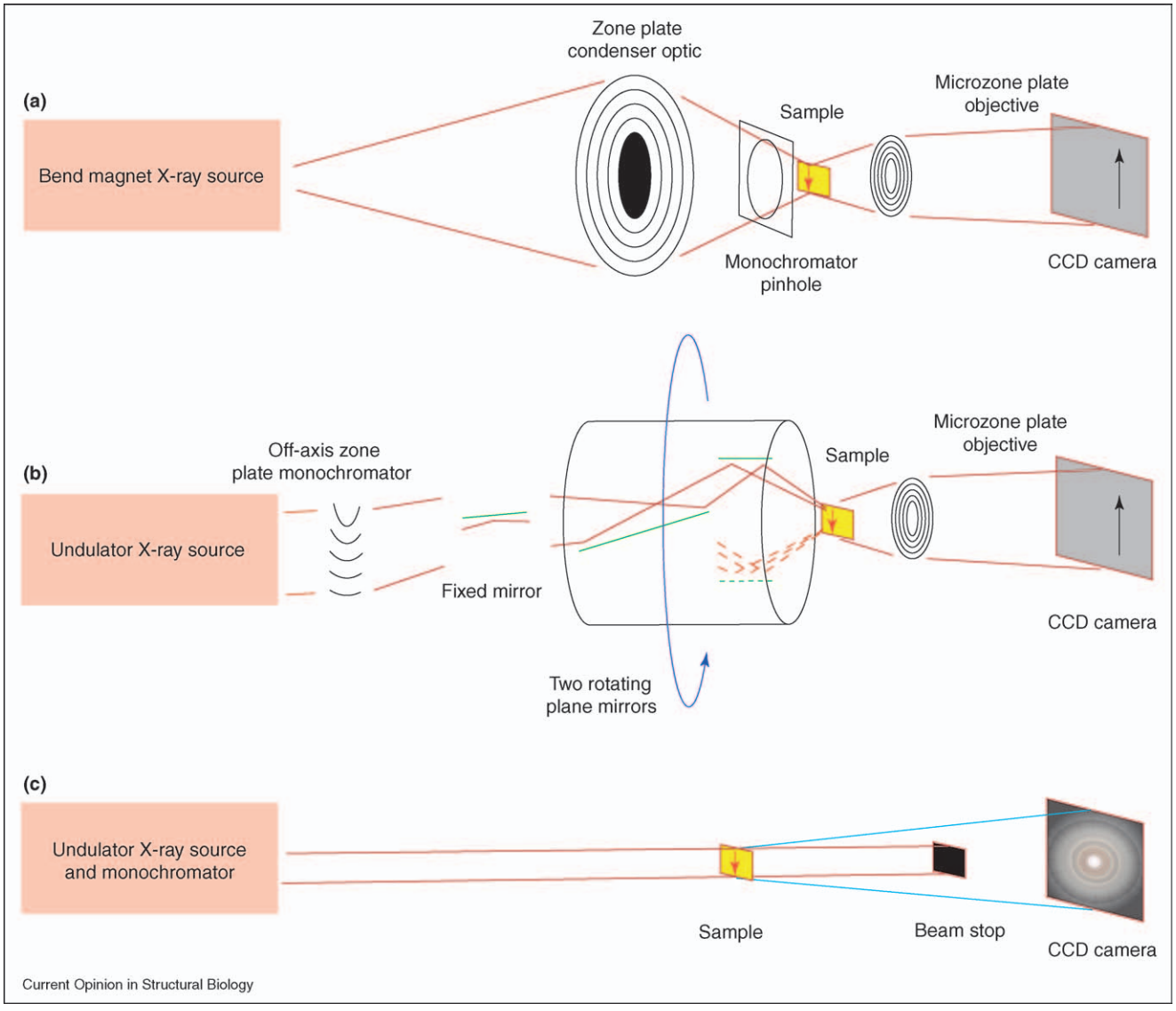

Schematics of X-ray microscopes used in cellular tomography. **(a)** Basic configuration of a bright field TXM with a zone plate condenser lens. Ideally, the optic used to focus X-rays onto the sample should have a numerical aperture equal to that of the objective imaging lens in order to optimize the full-field image quality. A microzone plate objective lens forms the magnified image of the sample on a CCD camera. The condenser also functions as a monochromator when combined with a 10 $\times$ 10 μm pinhole placed before the sample. The energy resolution obtained at 500 eV is $\sim$1 eV. The optimal source is a broad-bandwidth synchrotron bend magnet. Dark field and phase contrast configurations have also been demonstrated [16]. **(b)** A TXM that uses an alternative condenser optic. The rotating optical components produce a hollow cone illumination and also average the coherent flux produced by the undulator, thus preventing speckle artifacts in the image. The mirrors are not drawn to scale. The dashed component shows the position of the exit mirror after a 180° rotation of the condenser [15]. An off-axis zone plate acts as a monochromator and prevents higher diffraction orders from entering the rotating condenser. With this configuration, an energy resolution of $\sim$0.2 eV at 500 eV is possible. **(c)** A lensless DIM requires no focusing optics but needs a highly coherent and intense source of X-rays, such as radiation from an undulator or X-ray free electron laser. Diffracted X-rays are detected by a CCD camera (which must be protected from the intense undiffracted beam by a beam stop). The monochromaticity required depends on the sample thickness. Gratings or off-axis zone plates can be used as a monochromator [30•].

STXM. This makes it much better suited to tomographic measurements, even though radiation damage in TXM is greater due to the low-efficiency (~20%) zone plate objective lens placed between the sample and detector [9]. Figure 1a,b shows the basic configuration of the TXM geometry. The complete image is formed as a single snapshot using a cooled back-thinned charge-coupled device (CCD) camera; for existing instruments, a 2048 × 2048 pixel image with high contrast can be taken in less than a second. TXMs with zone plate condensers, Figures 1a and 2, are the current workhorses of single-cell tomography. The TXM currently in operation at the Advanced Light Source (ALS) in Berkeley [10,11] is an adaptation of an earlier microscope design operated at the German synchrotron light source BESSY I (Berliner Elektronenspeicherring-Gesellschaft für Synchrotronstrahlung) [12]. The ALS instrument (XM-1) is capable of high-throughput cryo-tomography by virtue of an automated sample stage (MA Le Gros *et al.*, patent pending). A new microscope, designed specifically for biological applications, is currently being constructed at the ALS. This instrument (XM-2) will operate over the spectral range 150 to 6 KeV, enabling visualization of hydrated cellular structures by imaging in the water window (Figure 2b). This microscope will also have a tunability range that will allow the use of virtually any element as a molecular label. Another new X-ray microscope, employing a rotating condenser instead of a zone plate and an undulator X-ray source rather than a bend magnet, has recently been completed at BESSY II [13]. This microscope should eventually surpass the performance of zone plate condenser instruments, in both spectral resolution and speed of imaging, but at the cost of being significantly more expensive and having much greater opto-mechanical complexity.

STXMs use a single zone plate to form a diffraction-limited focused spot on the sample. The image is formed by raster scanning the sample [14] or the zone plate [15]. The detector is typically a single-element photomultiplier that is sensitive to optical photons generated by an X-ray-sensitive scintillator, although other detection schemes have also been used [16]. STXMs are best matched to undulator sources. For chemical and elemental spectral imaging, a monochromator or grating with superb energy resolution, typically less than 0.1 eV, is also required. Image formation times are typically one to two orders of magnitude greater than with the TXM. A 1k × 1k TXM image requires less than 1 s exposure. An equivalent image requires an exposure of around 100 s in the STXM. New generation STXMs [17] are beginning to exhibit a spatial resolution similar to that obtained using TXMs; however, a useable low-temperature biological sample stage has yet to be developed. This, combined with the long image formation time, means that few tomographic measurements of whole cells have been performed [18]. Next generation sources, such as free electron lasers, combined with innovative microscope designs, could change this situation.

Cryogenic sample stages

For whole-cell imaging, the destructive effects of radiation damage must be attenuated by cryo-cooling [19]. Consequently, optimized cryo-tomography stages that

Figure 2

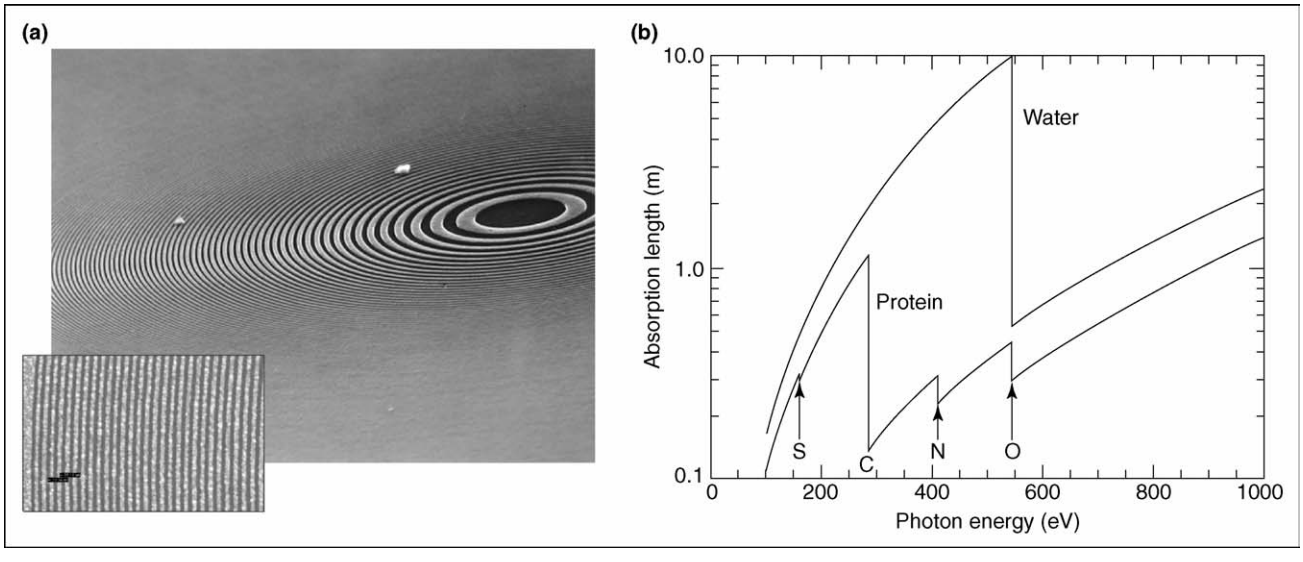

Zone plate optics and absorption contrast. **(a)** Fresnel zone plate for focusing soft X-rays, manufactured by patterning a large number of concentric rings on a substrate. The resolution achievable is dependent on the width of the outermost ring. An outer section of zone plate is shown in enlargement. Reproduced with permission from [9]. **(b)** Soft X-rays interact with matter by being absorbed or phase shifted. The graph shows the absorption length of a typical biological specimen (carbon 52.5%, oxygen 22.5%, nitrogen 16.5%, hydrogen 7.0%, sulfur 1.5%). For optimum water window imaging, photon energy just below the oxygen absorption edge is used. Reproduced with permission from [9].

permit isotropic data collection over 360° of rotation are desirable. In this regard, two approaches have been pursued, one involving the modification of the apparatus used for in-vacuum electron microscopy [18] and one involving the use of cold gas at atmospheric pressure [4,20,21]. Gas-based systems have been used to good effect to perform high-throughput cryo-tomography on a variety of samples. Figure 3a–c shows the cryo-tomography stage used at the ALS TXM. This stage is easily integrated with standard rapid freezing techniques, such as liquid propane plunge freezing. Modified versions are readily incorporated with optical microscopes, enabling sophisticated correlated X-ray and visible light imaging measurements of one sample (Figure 3d,e).

Figure 3

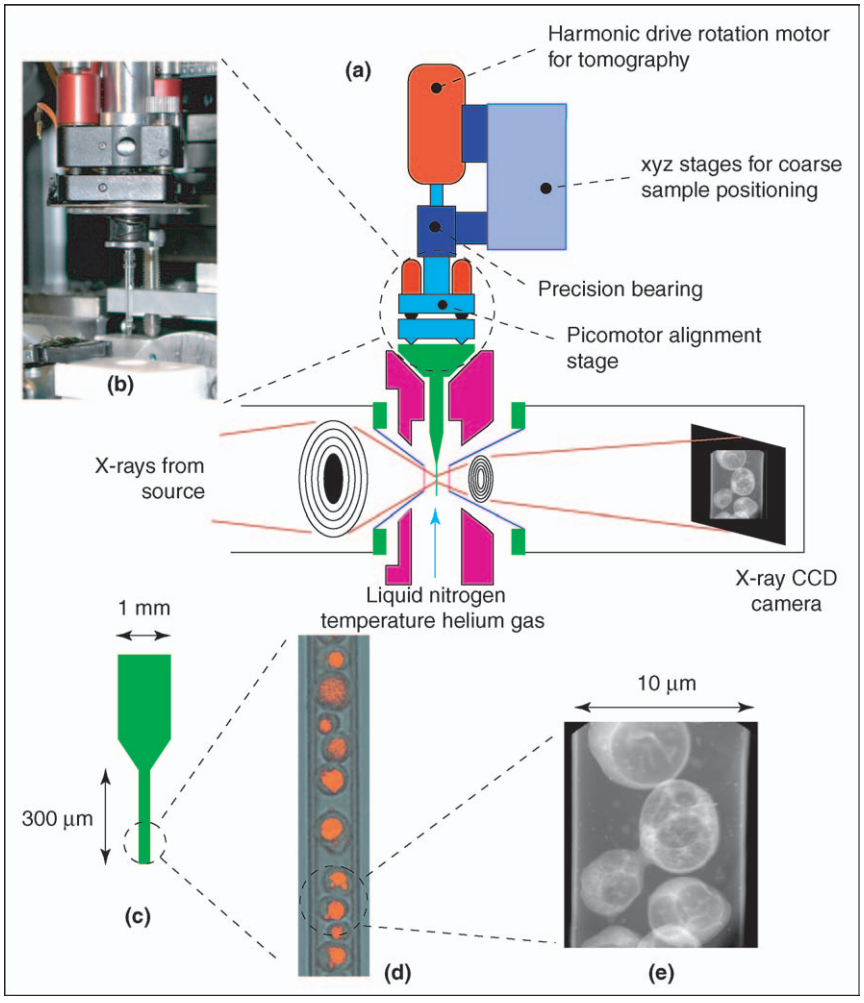

Cryo-rotation stage for a TXM. **(a)** Schematic of a cryogenic gas-based tomography stage, capable of being mounted on a soft X-ray TXM. The majority of the X-ray path is under high vacuum, including the condenser and objective zone plate lens. 100 nm thick silicon nitride windows mounted on low thermal conductivity cones separate the sample region from these vacuum spaces. Liquid-nitrogen-temperature helium gas continually flows over the sample to maintain low temperatures during imaging. The sample is mounted on an x,y,z θ stage and a motorized stage is used to center the region of interest on the rotation axis. This two-axis, picomotor-actuated stage is positioned above the sample tube and rotates with the sample. Centering is first performed using a light microscope to ensure that there is no more than 2 μm deviation as the sample is rotated through 180°. Further alignment is performed using a sequence of four low-dose X-ray images, which enables the rotation axis of the tomographic projection series to be positioned to better than 0.25 μm. The first alignment image is taken at 0° rotation and the position of the sample center is recorded. The sample is then rotated to 180°, the new position is noted and the axial alignment stage is used to position the sample at the mid point of the 0°/180° sample positions. The same procedure is used again for the 90°/270° sample positions. After this procedure, the sample is well aligned to the rotation axis of the cryo-stage, and a complete tomographic data set can be collected without any refocusing or translation of the sample. The entire alignment procedure can take less than 10 s and can easily be automated. The sample tubes are manufactured using a standard micropipette puller and are of sufficiently high symmetry that 50–100 μm of the tube length is suitable for the acquisition of a tomographic projection series after a single alignment procedure. **(b)** Close-up photograph of the sample alignment stage, with a capillary tube in place. **(c)** Schematic of a tomography sample capillary tube. **(d)** Dual channel fluorescence and bright field light microscope image of a typical sample. **(e)** X-ray micrograph of yeast in the end of the tube. Cell monolayer samples can also be studied using a 1 × 4 mm silicon nitride window as a specimen substrate.

Examples of whole-cell tomography using zone plate based microscopes

Other than cryo-cooling, whole-cell tomography using TXM has essentially no further sample preparation requirements. For example, this technique does not require exposing the cells to chemical fixatives or contrast enhancement reagents [8]. Therefore, the resultant tomogram is of a cell that closely resembles the native state. In practice, collection of tomographic data using this type of microscope is both simple and rapid. The capillary sample geometry also makes it possible to collect isotropic data over a 360° rotation range. This eliminates the loss of data that occurs in electron tomography; flat specimen holders can only be rotated ± 70° before they occlude the electron beam [22]. Because each capillary contains several cells (Figure 3d), it is possible to collect tomographic data sets in series by simply advancing the capillary along the rotation axis and bringing a new cell into the field of view.

During data collection, the yeast cells in Figure 4 were maintained at cryogenic temperatures using liquid-nitrogen-cooled helium gas. For each reconstruction, 45 full-field projection images were collected at 4° intervals over 180° of rotation. All 45 images were then aligned to a common axis of rotation, using the routine from the SPIDER [23] or IMOD [24] software suite of programs to align 60 nm diameter gold particle fiducials (arrows, Figure 4a). Figure 4a shows a single projection image of a typical field of view of a budding yeast cell. Although it is possible to see numerous overlapping vesicles and organelles inside the yeast, it is difficult to distinguish the precise boundaries of these organelles. However, tomographic reconstruction retrieves the three-dimensional information and reveals the internal structures of the cell (Figure 4b,c).

Once a three-dimensional map of the X-ray absorption coefficients was obtained, volume processing and visua-

Figure 4

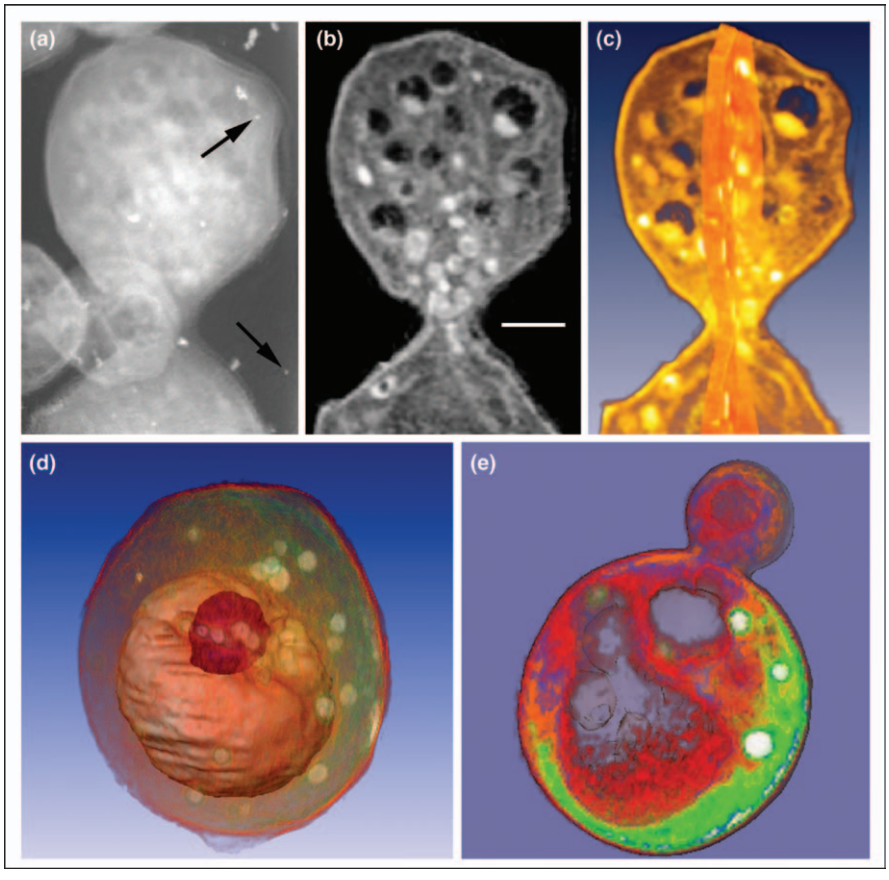

Tomography of whole yeast cells using TXM. **(a)** Single projection image of a rapidly frozen budding yeast. The data for the complete three-dimensional reconstruction were composed of 45 such images, collected through a total of 180° of rotation. **(b)** Computer-generated section through a tomographic reconstruction of the raw data shown in (a). The scale bar is 0.5 μm. **(c)** Cropped volume rendered view of the reconstructed data from (b). **(d)** An edge enhancement gradient algorithm was used to volume segment the three-dimensional data used to produce this volume rendered image, showing the nucleus (purple), vacuole (pink) and lipid droplets (white). **(e)** Color-coded reconstruction of a budding yeast. Lipid droplets, which are the densest structures, were color coded white, the least dense vacuoles were color coded gray, and numerous other subcellular structures of intermediate densities were colored shades of green, orange and red. All images similar to those published in [3••].

lization techniques were used to analyze the data [3••,25]. One such visualization algorithm was used to extract the surface of the yeast cell, revealing the internal structures, and edge enhancement algorithms were used to reveal numerous organelles (Figure 4d). The entire tomogram can be color coded based on the density of cellular structures, as determined by the volume-reconstructed X-ray absorption coefficients (Figure 4e). The tomographic reconstruction of *Escherichia coli* reveals absorbance differences indicative of complex structural details (Figure 5).

Lensless microscopes

Projection techniques are synchrotron-based high photon flux versions of conventional medical tomography that can produce tomographic reconstructions with a resolution approaching 2 μm for millimeter-scale objects. Impressive volume reconstructions of bone and other X-ray-absorbing biological materials have been demonstrated, but, to date, only low-resolution images of cellular tissue have been recorded [1,2].

Another form of lensless imaging is diffraction imaging of non-periodic objects, a new and exciting field [26]. The DIM method determines the two- and three-dimensional structures of nanocrystals and non-crystalline samples using coherent X-rays and electrons [27]. In this approach, coherent diffraction patterns are recorded (Figure 1c) and then converted directly into high-resolution images using the over-sampling phasing method. In conventional Bragg diffraction methods, the diffracted X-rays from multiple copies of the molecule constructively interfere to produce an intense signal. In the case of single particles, for which interference obviously does not occur, the diffraction patterns are usually very weak. In practice, diffraction imaging tomography of single cells is performed in a similar fashion to lens-based tomography [28] — the only difference being that, for each angle for which a projection diffraction pattern is formed, a computer algorithm is used to reconstruct the real space image, rather than using an optical element [26].

The DIM method is, in principle, an optimal method for X-ray imaging, as there is no intensity loss of high spatial frequency information due to a lens contrast transfer function. The theoretical resolution limit is close to the wavelength used to create the diffraction pattern. However, limitations concerning sample configuration (isolated particles are required) and long data acquisition times (many hours) make the technique fairly low-throughput compared to zone plate based X-ray microscopes. As with zone plate imaging, cryogenic sample stages must be used to help mitigate the effects of radiation damage during data collection. This technique is just beginning to produce biological images (Figure 6) [29] and will require much effort to prove that results similar to those obtained with zone plate instruments are possible. Establishment of the DIM method calls for significant further work on the development of image reconstruction methodologies and on other experimental

Figure 5

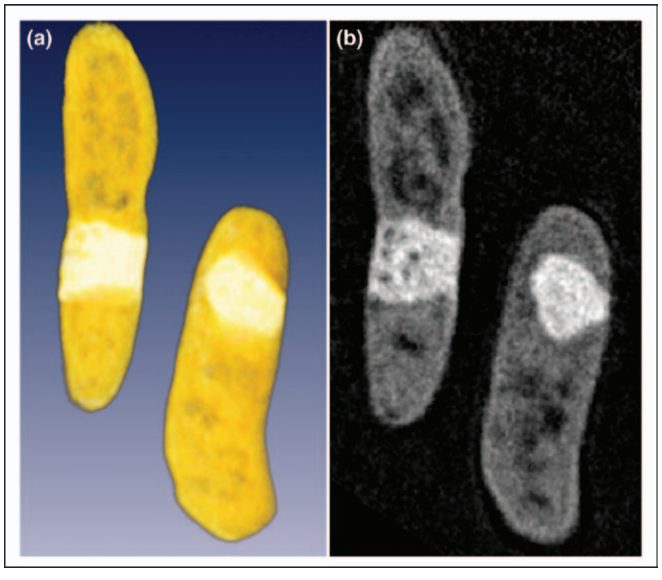

Tomography of whole bacteria cells using TXM. **(a)** Single projection image of rapidly frozen *E. coli*. The data for the complete three-dimensional reconstruction were composed of 45 such images, collected through a total of 180° of rotation. **(b)** Computer-generated section through a tomographic reconstruction of the raw data shown in (a). The X-ray absorption coefficients are colored light to dark — dark is most transparent and light most X-ray absorbing (and hence most dense). The exact nature of the dense region in both bacteria is not certain and is the subject of further work (CA Larabell and MA Le Gros, unpublished images).

Figure 6

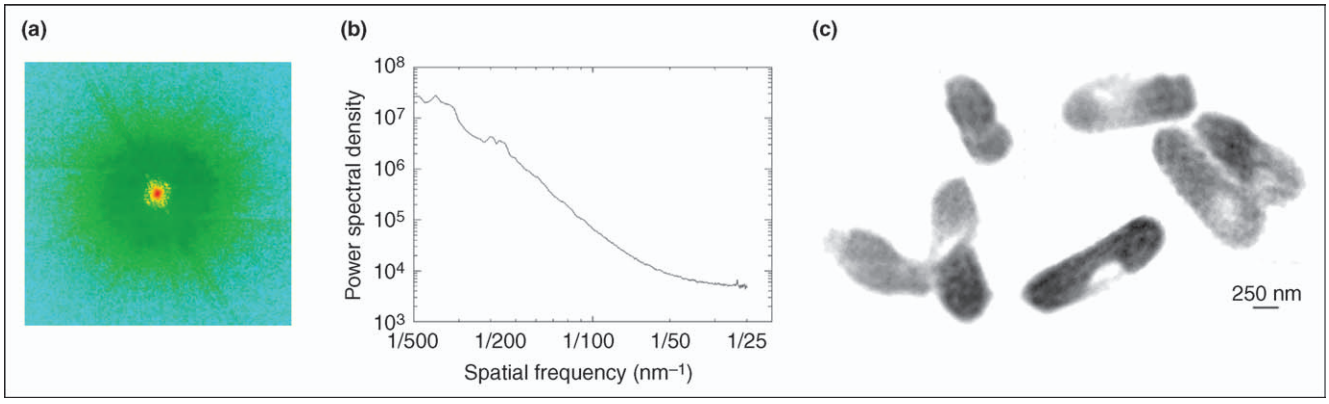

Image of whole bacteria using DIM. **(a)** Diffraction pattern (512 × 512 pixels) recorded from manganese-tagged *E. coli*. **(b)** The power spectral density of the diffraction pattern indicates that the resolution extends to 30 nm. The radiation dose to the sample was estimated to be ~8×10^6 Gray. According to previous experiments, this dose would make no appreciable structural changes to the sample. The diffraction pattern has an area of 70 × 70 pixels of low-resolution (~200 nm) missing data at the center, which was filled using the magnitude of the Fourier transform calculated from an X-ray microscopy image of the sample [29]. The missing data area, which is much larger than the size of the beam stop used to block the direct beam (~2 × 2 pixels), is mainly due to the low dynamic range of the CCD. This problem may be solved in the future by using area detectors with a high dynamic range and high quantum efficiency. Reproduced with permission from [29]. **(c)** Image of reconstructed *E. coli*. The dense regions inside the bacteria probably represent the distribution of proteins labeled with $KMnO_4$. Reproduced with permission from [29].

concerns, such as the effect of requiring a zero-order beam stop and the isolated object required for the over-sampling reconstruction methodology. Cryo-stages and sample holders for this type of imaging are practically identical to high-vacuum electron microscopy instrumentation. Gas-based cryogenic systems could not be used, because they would introduce too much non-specific scattering into the sample diffraction pattern.

Conclusions and outlook

Imaging the subcellular structure of a whole cell by X-ray methods has undergone a significant number of breakthroughs over the past three years. In addition to the publication of 'proof of concept' experiments, several new synchrotron-based biological X-ray microscopes are under construction.

Of the two main instrument types, full-field zone plate based microscopes have produced the most significant results. Operating in the water window, zone plate based X-ray tomography of whole cells has been demonstrated at a resolution of better than 50 nm. In the near future, the achievable resolution will be extended to between 10 and 15 nm. The advent of gas-based cryo-stages has mitigated the issue of radiation damage, and has made the technique high throughput and capable of producing many thousands of tomograms per year. Coupled with developments in labeling methods, it will soon be possible to collect statistically significant numbers of tomograms and, as a consequence, generate spatial and temporal maps that locate subcellular components during key cellular events. The number and type of biological problems that can be addressed using X-ray tomography is also expanding. The new generation of sample stages can also accommodate various sample types and thus opens up the possibility of examining flat or large samples, such as whole tumor nodules or whole embryos. There is also great potential for the development of multicolor X-ray probes that can be used to simultaneously localize multiple proteins within the cell. Overall, X-ray tomography of whole cells is coming of age. Current and future advances in instrumentation and experimental procedures will undoubtedly be the source of much exciting new science.

Acknowledgements

The authors thank Weiwei Gu for critical reading and discussion. This work was funded by the US Department of Energy, Office of Biological and Environmental Research (DE-AC02-05CH11231), the National Center for Research Resources of the National Institutes of Health (P41 RR019664-02) and the National Institutes of General Medicine of the National Institutes of Health (GM63948).

References and recommended reading

Papers of particular interest, published within the annual period of review, have been highlighted as:

- • of special interest
- •• of outstanding interest

1. Cloetens P, Baruchel J, Boivin G: **Quantification of the degree of mineralization of bone in three dimensions using synchrotron radiation microtomography**. *Med Phys* 2002, **29**:2672-2681.

2. Stock SR, Ignatiev KI, Dahl T, Veis A, De Carlo F: **Three-dimensional microarchitecture of the plates (primary, secondary, and carinar process) in the developing tooth of *Lytechinus variegatus* revealed by synchrotron X-ray absorption microtomography (microCT)**. *J Struct Biol* 2003, **144**:282-300.

3. •• Larabell CA, Le Gros MA: **X-ray tomography generates 3-D reconstructions of the yeast, *Saccharomyces cerevisiae*, at 60-nm resolution**. *Mol Biol Cell* 2004, **15**:957-962.

This paper presents the state of the art in high-resolution X-ray tomography of cryogenic whole-cell specimens. Movies of multiple tomographic data sets are available at ncxt.lbl.gov.

4. Schneider G, Anderson E, Vogt S, Knochel C, Weiss D, Le Gros M, Larabell C: **Computed tomography of cryogenic cells**. *Surf Rev Lett* 2002, **9**:177-183.

5. Weiss D, Schneider G, Vogt S, Guttmann P, Niemann B, Rudolph D, Schmahl G: **Tomographic imaging of biological specimens with the cryo transmission X-ray microscope**. *Nucl Instrum Methods Phys Res A* 2001, **467**:1308-1311.

6. •• Chao W, Harteneck B, Liddle JA, Anderson EH, Attwood D: **Sub-15 nm spatial resolution soft X-ray microscopy**. *Nature* 2005, **435**:1210-1213.
This paper presents a breakthrough fabrication technique for high-resolution zone plate optics and shows high-resolution data obtained from specially made test patterns.

7. Chapman HN, Jacobsen C, Williams S: **A characterisation of dark-field imaging of colloidal gold labels in a scanning transmission X-ray microscope**. *Ultramicroscopy* 1996, **62**:191-213.

8. Meyer-Ilse W, Hamamoto D, Nair A, Lelievre SA, Denbeaux G, Johnson L, Pearson AL, Yager D, Le Gros MA, Larabell CA: **High resolution protein localization using soft X-ray microscopy**. *J Microsc* 2001, **201**:395-403.

9. Attwood D: *Soft X-rays and Extreme Ultraviolet Radiation: Principles and Applications.* Cambridge: Cambridge University Press; 1999.

10. Meyer-Ilse W, Medecki H, Jochum L, Anderson E, Attwood D, Magowan C, Balhorn R, Moronne M, Rudolph D, Schmahl G: **New high-resolution zone-plate microscope at beamline 6.1 of the ALS**. *Synchrotron Radiation News* 1995, **8**:29-33.

11. Denbeaux G, Fischer P, Schneider G, Liddle JA, Anderson E, Pearson A, Chao W, Larabell C, Le Gros M, Attwood D: **Full-field soft X-ray microscopy at the Advanced Light Source**. *Synchrotron Radiation News* 2003, **16**:16-21.

12. Schmahl G, Rudolph D, Niemann B, Christ O: *The Goettingen X-ray Microscope and X-ray Microscopy Experiments at the BESSY Storage Ring*, vol 43. Edited by Schmahl G, Rudolph D. Springer Series in Optical Sciences; 1984.

13. Guttmann P, Niemann B, Thieme J, Hambach D, Schneider G, Wiesemann U, Rudolph D, Schmahl G: **Instrumentation advances with the new X-ray microscope at BESSY II**. *Nucl Instrum Methods Phys Res A* 2001, **857**:467-468.

14. Rarback H, Buckley C, Goncz K, Ade H, Anderson E, Attwood D, Batson P, Hellman S, Jacobsen C, Kern D: **The scanning transmission microscope at the NSLS**. *Nucl Instrum Methods Phys Res A* 1990, **291**:54.

15. Wiesemann U, Thieme J, Fruke R, Guttmann P, Niemann B, Rudolph D, Schmahl G: **Construction of a scanning transmission X-ray microscope at the undulator U-41 at BESSY II**. *Nucl Instrum Methods Phys Res A* 2001, **861**:467-468.

16. Vogt S, Chapman HN, Jacobsen C, Medenwaldt R: **Dark field X-ray microscopy: the effects of condenser/detector aperture**. *Ultramicroscopy* 2001, **87**:25-44.

17. Ade H, Kilcoyne ALD, Tyliszczak T, Hitchcock P, Anderson E, Harteneck B, Rightor EG, Mitchell GE, Hitchcock AP, Warwick T: **Scanning transmission X-ray microscopy at a bending magnet beamline at the Advanced Light Source**. *Journal de Physique IV* 2003, **104**:3-8.

18. Wang Y, Jacobsen C, Maser J, Osanna A: **Soft X-ray microscopy with a cryo scanning transmission X-ray microscope: II. Tomography**. *J Microsc* 2000, **197**:80-93.

19. Glaeser RM: **Low temperature electron microscopy - radiation damage in crystalline biological materials**. *J Microsc* 1971, **12**:133.

20. Weiss D, Schneider G, Niemann B, Guttmann P, Rudolph D, Schmahl G: **Computed tomography of cryogenic biological specimens based on X-ray microscopic images**. *Ultramicroscopy* 2000, **84**:185-197.

21. Larabell C, Le Gros M: **Whole cell cryo X-ray tomography and protein localization at 50 micron resolution**. *Biophys J* 2004, **86**:185A.

22. Baumeister W, Grimm R, Walz J: **Electron tomography of molecules and cells**. *Trends Cell Biol* 1999, **9**:81-85.

23. Frank J, Radermacher M, Penczek P, Zhu J, Li YH, Ladjadj M, Leith A: **Spider and web - processing and visualization of images in 3D electron microscopy and related fields**. *J Struct Biol* 1996, **116**:190-199.

24. Kremer JR, Mastronarde DN, McIntosh JR: **Computer visualization of three-dimensional image data using IMOD**. *J Struct Biol* 1996, **116**:71-76.

25. Frank J: *Electron Tomography*. New York: Plenum Press; 1992.

26. Miao J, Charalambous P, Kirz J, Sayre D: **Extending the methodology of X-ray crystallography to allow imaging of micrometre-sized non-crystalline specimens**. *Nature* 1999, **400**:342.

27. Miao J, Ohsuna T, Terasaki O, Hodgson KO, O'Keefe MA: **Atomic resolution three-dimensional electron diffraction microscopy**. *Phys Rev Lett* 2002, **89**:155502.

28. Miao J, Ishikawa T, Johnson B, Anderson EH, Lai B, Hodgson KO: **High resolution 3D X-ray diffraction microscopy**. *Phys Rev Lett* 2002, **89**:088303.

29. Miao J, Hodgson KO, Ishikawa T, Larabell CA, Le Gros MA, Nishino Y: **Imaging whole *Escherichia coli* bacteria by using single-particle X-ray diffraction**. *Proc Natl Acad Sci USA* 2003, **100**:110-112.

30. • Marchesini S, He H, Chapman HN, Hau-Riege SP, Noy A, Howells MR, Weierstall U, Spence JCH: **X-ray image reconstruction from a diffraction pattern alone**. *Phys Rev B* 2003, **68**:140101.
This paper introduces a new method for phasing a DIM pattern that does not require a low-resolution direct image of the object.